

LHC Signals of a Heavy CP-even Higgs Boson in the NMSSM via Decays into a Z and a Light CP-odd Higgs State

M. M. Almarashi and S. Moretti

School of Physics and Astronomy, University of Southampton, Highfield, Southampton SO17 1BJ, UK.

(Dated: July 10, 2018)

We study the Za_1 decay mode of a heavy CP-even Higgs boson of the NMSSM, h_2 , where a_1 is the lightest CP-odd Higgs state of this scenario, the former produced in association with a bottom-antibottom pair, and find that, despite small event rates, a significant (in fact essentially background free) signal should be extractable at the LHC with very high luminosity, so long that a $Z \rightarrow jj$ (where j represents a jet) and $a_1 \rightarrow \tau^+\tau^-$ final state is exploited, in presence of b -tagging.

PACS numbers:

The Next-to-Minimal Supersymmetric Standard Model (NMSSM) [1], owing to the introduction of an extra complex Higgs singlet field, which only couples to the two MSSM-type Higgs doublets, embeds a Higgs sector which comprises a total of seven mass eigenstates: a charged pair h^\pm , three CP-even Higgses $h_{1,2,3}$ ($m_{h_1} < m_{h_2} < m_{h_3}$) and two CP-odd Higgses $a_{1,2}$ ($m_{a_1} < m_{a_2}$).

Consequently, Higgs phenomenology in the NMSSM can be very different from that of the MSSM. As a key example, over the past few years, there have been several attempts to extend the so-called ‘No-lose theorem’ of the MSSM – stating that at least one MSSM Higgs boson should be observed through the usual SM-like production and decay channels at the Large Hadron Collider (LHC) throughout the entire MSSM parameter space [2] – to the case of the NMSSM [3–5]. From this perspective, it was realised that at least one NMSSM Higgs boson should remain observable at the LHC over the NMSSM parameter space that does not allow any Higgs-to-Higgs decay mode. In contrast, when a light non-singlet (and, therefore, potentially visible) CP-even Higgs boson, h_1 or h_2 , decays mainly to two very light CP-odd Higgs bosons, $h_{1,2} \rightarrow a_1 a_1$, one may not have any Higgs signal of statistical significance at the LHC [6]. In fact, further violations to the theorem may well occur if one enables Higgs-to-sparticle decays (e.g., into neutralino pairs, yielding invisible Higgs signals) [23]. While there is no conclusive evidence on whether a ‘No-lose theorem’ can be proved for the NMSSM at the LHC, there has also been put forward an orthogonal approach: to see when a, so to say, ‘More-to-gain theorem’ for the LHC [7–9] can be formulated within the NMSSM. That is, whether there exist regions of the NMSSM parameter space where more and/or different Higgs states are visible at the LHC than those available within the MSSM.

In our attempt to overview both such possibilities, we assume here a light CP-odd Higgs boson, a_1 , emerging from the decay $h_2 \rightarrow Za_1$, where the heavy CP-even state, h_2 , is produced in association with b -quark pairs at the LHC. This work complements the one carried out in a previous paper where the light a_1 state is produced in pairs from decays of not only h_2 states but also h_1 ones, always from the aforementioned production mode

[10]. Direct a_1 production in association with $b\bar{b}$ pairs was considered in [11] for the case of $a_1 \rightarrow \tau^+\tau^-$ as well as $a_1 \rightarrow \gamma\gamma$ decays, in [12] for the case of the $a_1 \rightarrow \mu^+\mu^-$ channel and in [13] for the $a_1 \rightarrow b\bar{b}$ mode.

For our study of the NMSSM Higgs sector we have used NMSSMTools [14, 15], which is a numerical package computing the masses, couplings and decay widths of all the Higgs bosons of the NMSSM in terms of its input parameters at the Electro-Weak (EW) scale. NMSSMTools also takes into account theoretical constraints as well as experimental limits, including the unconventional channels relevant for the NMSSM.

Here, instead of postulating unification or taking into account the SUSY breaking mechanism, we fix the soft SUSY breaking terms to a very high value, so that they give a small or no contribution at all to the outputs of the parameter scans. Consequently, we are left with six free parameters at the EW scale, uniquely defining the NMSSM Higgs sector at tree-level. Our parameter space is in particular identified through the Yukawa couplings λ and κ , the soft trilinear terms A_λ and A_κ , plus $\tan\beta$ (the ratio of the Vacuum Expectation Values (VEVs) of the two Higgs doublets) and $\mu_{\text{eff}} = \lambda\langle S \rangle$ (where $\langle S \rangle$ is the VEV of the Higgs singlet).

In order to make a comprehensive study of the NMSSM parameter space, we have used NMSSMTools to scan over the aforementioned six parameters taken in the following intervals:

$$\begin{aligned} 0.0001 < \lambda < 0.7, \quad 0 < \kappa < 0.65, \quad 1.6 < \tan\beta < 54, \\ 100 \text{ GeV} < \mu_{\text{eff}} < 1 \text{ TeV}, \quad -1 \text{ TeV} < A_\lambda < 1 \text{ TeV}, \\ -10 \text{ GeV} < A_\kappa < 0. \end{aligned}$$

Soft terms which are fixed in the scan include:

- $m_{Q_3} = m_{U_3} = m_{D_3} = m_{L_3} = m_{E_3} = 1 \text{ TeV}$,
- $A_{U_3} = A_{D_3} = A_{E_3} = 1.2 \text{ TeV}$,
- $m_Q = m_U = m_D = m_L = m_E = 1 \text{ TeV}$,
- $M_1 = M_2 = M_3 = 1.5 \text{ TeV}$.

We have finally performed our scan over 2×10^7 randomly selected points in the specified parameter space. The points which violate the constraints (either theoretical or experimental) are automatically eliminated by NMSSMTools.

The surviving data points are then used to determine the cross-sections for NMSSM Higgs hadro-production by using CalcHEP [16] for signals and MadGraph [17] for backgrounds. As the SUSY mass scales have been arbitrarily set well above the EW one (see above), the NMSSM Higgs production modes exploitable in simulations at the LHC are those involving couplings to heavy ordinary matter only. Amongst the productions channels onset by the latter, we focus here on

$$pp(q\bar{q}, gg) \rightarrow b\bar{b} h_2, \quad (1)$$

i.e., Higgs production in association with a b -quark pair, followed by

$$h_2 \rightarrow Za_1 \quad (2)$$

(incidentally, notice that h_1 is never heavy enough to enable sizable Za_1 decays) and then

$$Za_1 \rightarrow (jj)(\tau^+\tau^-) \text{ (where } j = \text{jet)}. \quad (3)$$

Notice that we discard here the possibility of $a_1 \rightarrow \mu^+\mu^-$ decays, for two reasons: on the one hand, the mass region below the $\tau^+\tau^-$ threshold is severely constrained (see [18] and references therein); on the other hand, the $\mu^+\mu^-$ decay rates are $\approx (m_\mu^{\text{pole}}/m_\tau^{\text{pole}})^2$ times suppressed with respect to the $\tau^+\tau^-$ ones, so that they would be numerically irrelevant (see forthcoming figures). As for $a_1 \rightarrow b\bar{b}$ decays, while being in turn more numerous than the $\tau^+\tau^-$ ones (above the $2m_b$ threshold) by an amount $\propto (m_b(m_{h_2})/m_\tau^{\text{pole}})^2$, they are overwhelmed by QCD backgrounds in Z +jet final states. Notice that the a_1 masses of relevance to this study will typically range between 15 and 60 GeV or so.

We adopt herein CTEQ6L [19] as parton distribution functions, with scale $Q = \sqrt{s}$, the centre-of-mass energy at parton level, for all processes computed. We finally assume $\sqrt{s} = 14$ TeV throughout for the LHC energy. Also, in our numerical analyses, we have taken $m_b(m_b) = 4.214$ GeV and $m_t^{\text{pole}} = 171.4$ GeV for the (running) bottom- and (pole) top-quark mass, respectively, while we have input $m_\tau^{\text{pole}} = 1.777$ GeV and $m_\mu^{\text{pole}} = 0.1057$ GeV for the (pole) tau- and (pole) muon-lepton mass, respectively.

As an initial step towards the analysis of the data, we have computed the production cross-section $\sigma(pp \rightarrow b\bar{b}h_2)$ times the decay $\text{BR}(h_2 \rightarrow Za_1)$ against the BR itself, see Fig. 1. It is clear from this plot that most of the NMSSM parameter space yields rather small rates: in fact, only when the $\text{BR}(h_2 \rightarrow Za_1)$ is large the overall process (1)–(2) can offer some chances of detection. In this scatter plot, one can notice a population of points with cross-section of up to several pb's. This region of parameter space is the only one exploitable at the LHC and reflects a well defined setup for the six input parameters of the NMSSM. Generally, such points correspond to generic and comfortably perturbative λ and κ (between 0.05 and 0.15), very large $\tan\beta$ (above 35), rather large

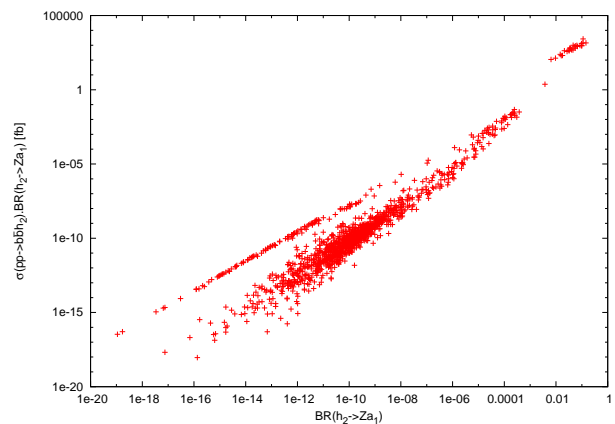


FIG. 1: $\sigma(pp \rightarrow b\bar{b}h_2) \text{BR}(h_2 \rightarrow Za_1)$ vs. $\text{BR}(h_2 \rightarrow Za_1)$.

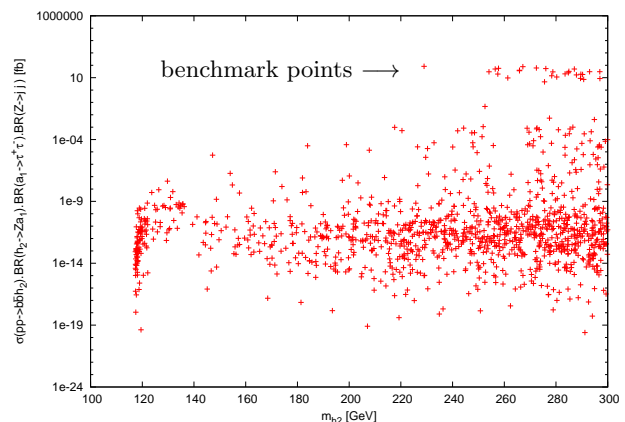


FIG. 2: $\sigma(pp \rightarrow b\bar{b}h_2) \text{BR}(h_2 \rightarrow Za_1) \text{BR}(a_1 \rightarrow \tau^+\tau^-) \text{BR}(Z \rightarrow jj)$ vs m_{h_2} .

(and positive) μ_{eff} and large (and negative) A_λ (both between 200 and 900 GeV) and slightly negative A_κ (between -10 and -1 GeV).

The rates in the previous figure refer to on-shell Z and a_1 though. One should clearly extract these from suitable decays, inevitably coming with a decay probability less than 1. Here, as intimated earlier on, we attempt the case of hadronic decays of the gauge boson and τ -decays of the CP-odd Higgs boson. The corresponding signal yield for the ensuing final state is displayed in Fig. 2, now mapped against m_{h_2} . After folding in the above decay probabilities, one is left with event rates at the $\mathcal{O}(100)$ fb level at the most. While clearly this number is not very large, signal events may still be detectable at planned LHC luminosities, especially if the background can be successfully reduced to manageable levels. Before proceeding to do so, it is worth mentioning that this kind of event rates are only found for h_2 masses well above 250 GeV.

We perform next a partonic signal-to-background (S/B) analysis. Amongst the backgrounds, we con-

Point	λ	κ	$\tan\beta$
1	0.11784333E+00	0.99759129E-01	0.45413385E+02
2	0.36954734E-01	0.74106016E-01	0.35731787E+02
3	0.55822718E-01	0.41921611E-01	0.47269331E+02
4	0.15630654E+00	0.84945744E-01	0.48122165E+02

Point	μ_{eff} [GeV]	A_λ [GeV]	A_κ [GeV]
1	0.65363068E+03	-0.56108302E+03	-0.97511471E+01
2	0.33852788E+03	-0.68364824E+03	-0.13135077E+01
3	0.38990121E+03	-0.29909449E+03	-0.53814631E+01
4	0.42293377E+03	-0.23627361E+03	-0.74575765E+01

Point	m_{a_1} [GeV]	m_{h_2} [GeV]	Γ_{a_1} [GeV]	Γ_{h_2} [GeV]
1	44.1	272.4	0.205	6.57
2	15.9	261.4	0.01879	4.972
3	61.5	275.6	0.00293	7.86
4	31.9	287.9	0.0674	8.37

Point	$\sigma(pp \rightarrow b\bar{b}h_2)$	$\text{BR}(h_2 \rightarrow Za_1)$ [fb]	$\text{BR}(a_1 \rightarrow \tau^+\tau^-)$
1		1286.35	0.141549576
2		377.3	0.07615127
3		109.0	0.125658544
4		447.1	0.111203597

TABLE I: The NMSSM benchmark points used in the S/B analysis.

consider here what we verified to be the dominant one, the irreducible noise induced by $pp \rightarrow b\bar{b}Z\tau^+\tau^-$ channels (amounting to 60 Feynman diagrams in the unitary gauge). As benchmarks for the S/B analysis we have chosen four points in the above parameter space region (see Fig. 2), as illustrative examples. These benchmarks are given in Tab. I.

In the light of the cross-section and decay rates in the table, and recalling that $\text{BR}(Z \rightarrow jj) \approx 70\%$, the total inclusive cross-section for the signal in (1)–(3) for point 1(2)[3]{4} is 127(20)[10]{35} fb. The SM irreducible background inclusive rate is 7.6 fb. After implementing the following acceptance cuts [24]

$$\Delta R(i, j) > 0.4 \quad (i, j = b, \bar{b}, j, j, \tau^+\tau^-),$$

$$|\eta(i)| < 2.5 \quad (i = b, \bar{b}, j, j, \tau^+\tau^-),$$

$$p_T(i) > 15 \text{ GeV} \quad (i = b, \bar{b}, j, j, \tau^+, \tau^-), \quad (4)$$

and the selection ones as well

$$|M_{jj} - M_Z| < 15 \text{ GeV}, \quad |M_{\tau^+\tau^-} - m_{a_1}| < 15 \text{ GeV} \quad (5)$$

(wherein m_{a_1} need not be known beforehand, as it would be seen in the reconstructed $M_{\tau^+\tau^-}$ distribution: here it assumes the values of Tab. I), we obtain for the signal cross-sections the values 2.27(0.12)[0.21]{0.65} fb for point 1(2)[3]{4} so that the typical signal efficiency is approximately 1.78(0.57)[2.21]{1.87}%, respectively [25].

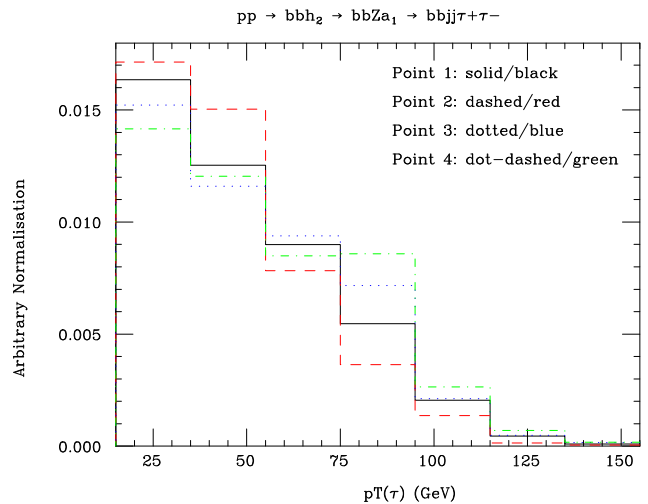


FIG. 3: The (reconstructed) τ transverse momentum distribution for the four benchmark points in Tab. I.

The selection efficiency strongly depends on the m_{a_1} value, see Fig. 3, in the sense that the lighter a_1 the softer its decay products (the $\tau^+\tau^-$ pair), so that the $p_T(\tau^+, \tau^-)$ selects fewer signal events: recall in fact that one has $m_{a_1} = 44.1(15.9)[61.5]\{31.9\}$ GeV for point 1(2)[3]{4}. Notice that after all such constraints the SM irreducible background is essentially removed altogether, as its rate goes down dramatically, to $\mathcal{O}(10^{-4})$ fb for all points 1–4. The distributions in invariant mass $m_{jj\tau^+\tau^-}$, that one could obtain after reconstructing the τ decay products, for the four benchmark points, are given in Fig. 4, showing the Breit-Wigner peaks signaling the $h_2 \rightarrow Za_1$ resonances. Integrating over the entire spectrum, one obtains 2274(115)[213]{653} signal events for point 1(2)[3]{4}, essentially background free, assuming 1000 fb^{-1} of integrated luminosity.

In summary, we have proven that there exists a small but well defined region of parameter space where the h_2 and a_1 states of the NMSSM, both with a mixed singlet and doublet nature, could potentially be detected at the LHC if $250 \text{ GeV} \lesssim m_{h_2} \lesssim 300 \text{ GeV}$ and $15 \text{ GeV} \lesssim m_{a_1} \lesssim 60 \text{ GeV}$, in the $h_2 \rightarrow Za_1 \rightarrow jj\tau^+\tau^-$ mode, when the CP-even Higgs state is produced in association with a $b\bar{b}$ pair for rather large $\tan\beta$, large (and positive) μ_{eff} , large (and negative) A_λ , and slightly negative A_κ , for typically perturbative values of λ and κ . After a realistic S/B analysis at parton level, we have in fact produced results showing that the extraction of such a signal above the dominant irreducible SM background should be feasible using standard reconstruction techniques [20, 21] and large LHC luminosities, i.e., after several years of running at design values or rather promptly at the Super-LHC [22]. While more refined analyses, incorporating τ -decays, parton shower, hadronisation and detector effects, are needed in order to delineate the true discovery potential of the LHC over the actual NMSSM parameter space, we are confident that our results are a

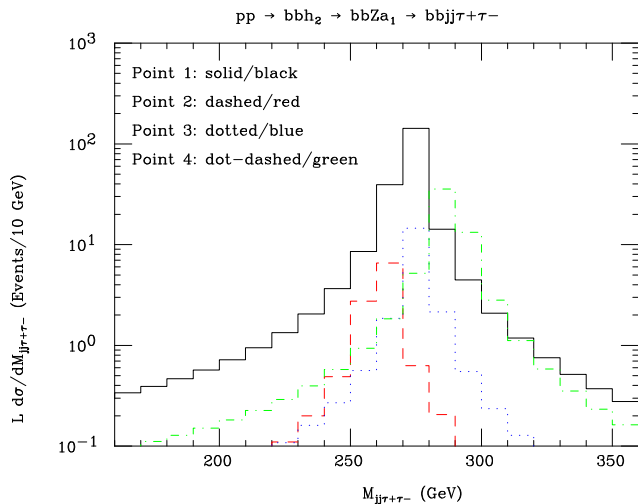


FIG. 4: The (reconstructed) h_2 mass peaks in terms of the $jj\tau^+\tau^-$ invariant mass distribution for the four benchmark points in Tab. I. We plot the number of events after an integrated luminosity $L = 1000 \text{ fb}^{-1}$.

step in the right direction to both: (i) prove the existence of a ‘More-to-gain theorem’ at the CERN collider for the NMSSM with respect to the MSSM (as Higgs $\rightarrow Z$ Higgs’ signals are only possible in the latter scenario in parameter space regions already excluded by experimental data) and (ii) to establish a ‘No-lose theorem’ for the NMSSM at the LHC (as some of the parameter regions where the aforementioned signal can be detected overlap with those where $h_{1,2} \rightarrow a_1 a_1$ decays might be ineffective in extracting an NMSSM Higgs signal).

Acknowledgments

This work is supported in part by the NExT Institute. M. M. A. acknowledges funding from Taibah University (Saudi Arabia).

-
- [1] For reviews, see: e.g., U. Ellwanger, C. Hugonie and A. M. Teixeira, *Phys. Rept.* **496** (2010) 1 (and references therein); M. Maniatis, *Int. J. Mod. Phys. A* **25** (2010) 3505 (and references therein).
- [2] J. Dai, J.F. Gunion and R. Vega, *Phys. Lett. B* **315** (1993) 355 and *Phys. Lett. B* **345** (1995) 29; J.R. Espinosa and J.F. Gunion, *Phys. Rev. Lett.* **82** (1999) 1084.
- [3] U. Ellwanger, J. F. Gunion and C. Hugonie, *JHEP* **0507** (2005) 041; U. Ellwanger, J.F. Gunion, C. Hugonie and S. Moretti, *hep-ph/0305109* and *hep-ph/0401228*.
- [4] U. Ellwanger, J.F. Gunion and C. Hugonie, *hep-ph/0111179*; D.J. Miller and S. Moretti, *hep-ph/0403137*; C. Hugonie and S. Moretti, *hep-ph/0110241*; A. Belyaev, S. Hesselbach, S. Lehti, S. Moretti, A. Nikitenko and C. H. Shepherd-Themistocleous, *arXiv:0805.3505* [hep-ph]; J. R. Forshaw, J. F. Gunion, L. Hodgkinson, A. Papaefstathiou and A. D. Pilkington, *JHEP* **0804** (2008) 090; A. Belyaev, J. Pivarski, A. Safonov, S. Senkin and A. Tatarinov, *Phys. Rev. D* **81** (2010) 075021.
- [5] S. Moretti, S. Munir and P. Poulose, *Phys. Lett. B* **644** (2007) 241.
- [6] D. Zerwas and S. Baffioni, private communication; S. Baffioni, talk presented at ‘GdR Supersymétrie 2004, 5-7 July 2004, Clermont-Ferrand, France.
- [7] S. Moretti and S. Munir, *Eur. Phys. J. C* **47** (2006) 791.
- [8] S. Munir, talk given at the ‘International School of Sub-nuclear Physics, 43rd Course’, Erice, Italy, August 29 – Sept. 7, 2005, to be published in the proceedings, preprint SHEP-05-37, October 2005.
- [9] E. Accomando *et al.*, *arXiv:hep-ph/0608079*.
- [10] M. M. Almarashi and S. Moretti, *Phys. Rev. D* **84** (2011) 035009.
- [11] M. M. Almarashi and S. Moretti, *Eur. Phys. J. C* **71** (2011) 1618.
- [12] M. M. Almarashi and S. Moretti, *Phys. Rev. D* **83** (2011) 035023.
- [13] M. M. Almarashi and S. Moretti, *Phys. Rev. D* **84** (2011) 015014.
- [14] U. Ellwanger, J.F. Gunion and C. Hugonie, *JHEP* **0502** (2005) 066; U. Ellwanger and C. Hugonie, *Comput. Phys. Commun.* **175** (2006) 290.
- [15] <http://www.th.u-psud.fr/NMHDECAY/nmssmtools.html>.
- [16] A. Pukhov, *arXiv:hep-ph/0412191*.
- [17] T. Stelzer and W. F. Long, *Comput. Phys. Commun.* **81** (1994) 357.
- [18] S. Andreas, O. Lebedev, S. R. Sanchez and A. Ringwald, *JHEP* **1008** (2010) 003.
- [19] <http://hep.pa.msu.edu/cteq/public/cteq6.html>.
- [20] ATLAS Collaboration, *arXiv:0901.0512* [hep-ex].
- [21] CMS Collaboration, *J. Phys. G* **34** (2007) 995.
- [22] F. Gianotti *et al.*, *Eur. Phys. J. C* **39** (2005) 293.
- [23] A sparticle is the Supersymmetry (SUSY) partner of an ordinary particle.
- [24] Here, for the sake of illustration, we take the τ ’s on-shell.
- [25] This includes a factor ε_b for each of the two b -tags which would be required (typically, $\varepsilon = 60\%$ for the above cut in $p_T(b, \bar{b})$) to isolate the signal we have discussed. Notice that to require to tag both b ’s in the final state with transverse momentum above 15 GeV induces a reduction of the signal cross sections, for the m_{h_2} values considered here, of about 7%, see Fig. 9 of [10].